EXPERIMENTAL TESTS RELATED TO THE MULTI-LAYERED BALLISTIC PANEL BEHAVIOUR UNDER BLAST AND FRAGMENTS IMPACT

Bogdan IFTIMIE[1], Alexandru-Cătalin CASAPU[2], Marin LUPOAE[3*], Florina BUCUR[4], Eugen TRANĂ[5]

The paper presents the results obtained from tests conducted to determine the influence of the characteristics of granular materials and the optimal configurations of arranging these materials together with layers of polyethylene based composite laminate, Dyneema HB24, in a multi-layer ballistic panel designed to attenuate the effects of shock waves and fragments resulting from the detonation of an Improvised Explosive Device (IED). The materials considered for testing and arranged in layers within the ballistic panel were sand, steel slag, and Dyneema fabric. The tests were initially performed on small-sized panels (500 mm x 500 mm) composed of layers of sand and steel slag, as well as Dyneema layers, to establish the influence of the particle size and thickness of granular and Dyneema layers on the attenuation of fragment and shrapnel velocities. For the conducted experimental tests, metal balls with diameters of 8 mm and 10 mm were used, propelled by an explosive device, along with Full Metal Jacket (FMJ) and Hollow Point Boat Tail (HPBT) bullets of 7.62 mm calibre. The results obtained in this phase were used to create a multi-layer ballistic panel with dimensions of 3 m x 2 m x 0.12 m, on which tests were conducted to determine the attenuation capacity of the effects of the IED explosion. For this panel, two assemblies consisting of 10 layers of Dyneema fabric positioned on either side of a 10 cm thick layer of slag were used, all arranged between Tego plates fixed to a metal structure. The obtained results showed that such a configuration of using granular materials and Dyneema fabric ensures complete attenuation of the velocities of fragments that can be propelled in the aftermath of an IED explosion.

Keywords: multi-layered ballistic panel, fragments mitigation, Dyneema, sand, steel slag

1. Introduction

The current global situation calls for a continuous focus on the development of ballistic protection systems that can be employed in various configurations and spaces.

[1, 2] PhD student, Military Technical Academy "Ferdinand I", Bucharest, Romania
[3*] Prof., Civil and Military Engineering and Geomatics Department, Military Technical Academy "Ferdinand I", Bucharest, Romania, corresponding author, e-mail: marin.lupoae@mta.ro
[4] Asocc. Prof., Mechatronics and Integrated Armament Systems Department, Military Technical Academy "Ferdinand I", Bucharest, Romania
[5] Prof., Mechatronics and Integrated Armament Systems Department, Military Technical Academy "Ferdinand I", Bucharest, Romania

The use of Improvised Explosive Devices (IEDs) by terrorists [1-4] in crowded spaces can cause significant destruction of material goods and loss of human lives [5-7]. Research on such ballistic panels that can be deployed in large open spaces with crowds [8-10] indicates that they possess certain special characteristics, such as [10]: i) large size, to mitigate the effects of an IED explosion as much as possible; ii) the necessity of using granular materials to achieve acceptable costs given their dimensions; iii) a symmetrical arrangement of layers within the panel; iv) the ability to be rapidly and easily maneuvered, with the possibility of integration into the architecture of the space where they are intended for use. Using shock polar methods for sand and Dyneema, Iftimie et al. [10] demonstrated that the optimal arrangement of sand and Dyneema layers for shock wave and fragment attenuation involves placing the granular material layer in the middle and the Dyneema layers on either side. Among the primary effects of an IED explosion, the most challenging to attenuate is the impact of fragments and shrapnel.

The behaviour of granular materials, particularly sand, subjected to the impact of projectiles, is extensively studied in the specialized literature [11-14]. Therefore, Børvik et al. [13] conducted experiments using dry and wet sand, as well as gravel, crushed stone, and rock with varying granulation. They subjected these materials to the impact of 7.62 mm and 12.5 mm Ball and AP bullets. Their findings revealed that the depth of penetration is influenced by the size of the granular material and whether the core fractures upon impact. The study also highlighted that energy dissipation during penetration occurs due to friction between particles and between particles and the bullet body.

Chian et al. [14] determined the ballistic limits and energy absorption as a function of impact velocity for projectiles with different nose shapes: spherical, semi-spherical, flat, and conical. The results of the experimental tests showed that the projectile's mass is a more important factor than the shape of the projectile's nose in terms of penetration resistance of granular materials. Chian et al. [14] also demonstrated that, for the same impact velocity, the absorbed energy by a spherical or semi-spherical projectile depends on the projectile's mass, with an increase in absorbed energy as the mass of the projectile increases.

However, the literature data analysed did not allow the establishing of a thickness of the granular material layer that attenuates a projectile with a specific impact velocity and a specific nose shape. Under these conditions, this study aims to present the results of experimental tests conducted to determine the residual velocity of projectiles based on the thickness of the granular material layer and layers of Dyneema fabric. The explosion of an IED can result in fragments of different masses and shapes, so metal balls were chosen for use in the tests to simulate these fragments as is stated by the Iftimie et al. in paper [9]. Due to their shape and homogeneity, these balls will be propelled by an explosive device at the highest velocity among all possible fragments, for the same fragment mass and the

same explosive mass. However, explosive devices for propelling metal balls cannot provide the repeatability conditions required for experimental tests. Therefore, for the initial phase of the tests, they were replaced with small-calibre firearm ammunition, namely HPBT and FMJ ammunition of 7.62 mm calibre.

Initial tests on small-sized panels (50 cm x 50 cm) allowed to determinate the influence of the type and granulation of sand and blast steel slag materials, with tests conducted on thicknesses of granular material layers up to 5 cm. After establishing the most effective type of sand and slag, experimental investigations continued to determine the dependence of residual velocity on the thickness of the granular material layer. By comparing the experimental data obtained with those from Chian et al. [14], a thickness of the slag layer necessary for attenuating 10 mm diameter metal balls to approximately 10 cm was determined. Experimental tests in a real configuration were conducted on full-scale multi-layer ballistic panels and confirmed their ability to attenuate fragments propelled by the explosion of an IED.

2. Materials and Methods

2.1. Granular materials

For the fabrication of ballistic panels employed in attenuating fragment and shrapnel velocities, the following materials were utilized, and their characteristics are presented in Fig. 1 and Table 1:

- sands of various granulations and moisture content;
- ash steel slag (resulting from steel production) of diverse granulations;
- layers of Dyneema fabric.

Table 1

The characteristics of the granular materials

No	Granular material type	Granulation, (mm)	Density, (kg/m^3)	Humidity, %
1.	Sand *0.4÷0.8 mm*	0.4 ÷ 0.8	1414	normal*
2.	Sand *max 1 mm*	max. 1	1456	normal*
			1077	5
			1131	10
			1162	15
3.	Steel slag	bulk	1773	normal*
		< 2	1972	
		2 ÷ 4	1606	
		4 ÷ 7	1559	

*) Material exposed to sunlight and subsequently packaged and stored under normal humidity conditions.

For the bulk steel slag, the distribution across various particle sizes was determined, resulting in a percentage of 29.71% for particles smaller than 2 mm, 33.95% for particles with diameters between 2 mm and 4 mm, 32.62% for particles with diameters between 4 mm and 7 mm, and 3.72% for particles with diameters greater than 7 mm.

a) sand 0.4÷0.8 mm | b) sand max 1mm | e) steel slag ϕ <2mm | f) steel slag 2mm< ϕ <4mm | g) steel slag 4mm< ϕ <7mm | h) bulk steel slag

Fig. 1. Types of granular materials used for the panels

2.2. Dyneema fabric

For experimental tests there was used a fabric of the Dyneema type HB24 (Ultra-High Molecular Weight Polyethylene based composite laminate) with an area density of 257-271 g/m^2. A layer of fabric consists of four single layers of unidirectional sheet cross plied at 90º to each other and consolidated with a polyurethane (PUR) based matrix. To assess their ability to attenuate the velocity of metal balls propelled by explosive devices, 6 to 10 layers of fabric were employed, fixed to a wooden frame, as illustrated in Fig. 3d.

2.3 The configuration for testing the attenuation capacity of projectile velocities

For the experimental tests, two testing configurations were employed, depending on the type of panels used, as depicted in Fig. 2:

- testing configuration for panels with dimensions of 50 cm x 50 cm, consisting of a panel made of granular material and/or granular material with layers of Dyneema, a high-speed camera and a ballistic radar, as shown in Fig. 2a.
- testing configuration for full-scale panels measuring 3 m x 2m x 0.12 m, composed of a multi-layer ballistic panel, explosive charge, a high-speed camera, a setup for measuring the pressure in the shock wave front, and a witness panel, as illustrated in Fig. 2b.

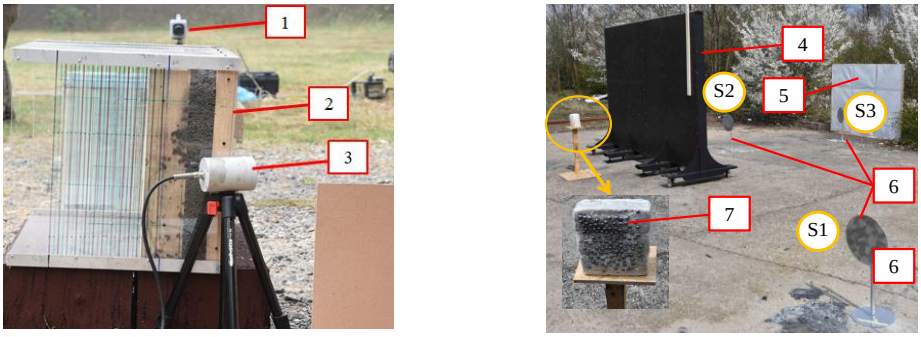

a) Testing setup for small-sized panels b) Testing setup for real-sized panels

Fig. 2. Testing setup for multi-layer ballistic panels: 1 – high-speed camera; 2 – panel with adjustable thickness for testing granular materials; 3 – ballistic radar; 4 – ballistic panel; 5 – witness panel; 6 – pressure sensor supports; 7 – explosive charge with metallic balls; S1, S2, S3 – pressure sensors

To fabricate the smaller-sized panels, frames made of wood, enclosed by 4 mm thick polycarbonate plates, 3 mm thick particleboard (PFL) plates, or 4 mm thick Tego (plywood for formwork) plates were manufactured, as depicted in Fig. 3a and 3b. Granular material was poured into the resulting boxes, and in some cases, layers of Dyneema fabric were arranged on the two sides. This type of box allowed the production of panels with interior thicknesses ranging from 3 cm to 5 cm. To prevent the deformation of polycarbonate and PFL boxes during the filling with granular material, hardwood spacers were installed between the plates.

a) box with polycarbonate plates | b) box with Tego plates | c) plexiglas box | d) panel with layers of Dyneema fabric

Fig. 3. Boxes/frames made of wood used for the fabrication of small-sized ballistic panels

To avoid deformation of the box walls when using granular material layers thicker than 5 cm, a Plexiglas box was constructed with cross-sectional dimensions of 50 cm x 50 cm and a depth of 40 cm, as shown in Fig. 3c. The front and rear walls were made of 10 mm thick Tego plates and a window with dimensions of 10 cm x 10 cm was cut in the centre of each wall, as depicted in Fig. 3c.
These windows were then covered with 10 cm x 10 cm Tego plywood plates, which were changed after 4 - 8 shots for the front sheet and 2 - 4 shots for the rear sheet to prevent the outflow of granular material. The rear wall was movable, and by displacing it, the thickness of the granular material layer could be adjusted.

For testing the shrapnel attenuation capacity by Dyneema fabric, wooden panels measuring 50 cm x 50 cm were fabricated, on which multiple layers (6, 10, or 12) of Dyneema were fixed, as depicted in Fig. 3d. For the propulsion of the balls, cylindrical devices with plastic explosive were employed, positioned at a distance of 50 cm from the panels. Further details regarding the explosive devices used for ball propulsion can be found in the paper Iftimie et al. [9].

2.4. Configuration for testing a multi-layer ballistic panel

To validate the results obtained from experiments on the small-sized multi-layer panels, a configuration for a full-scale multi-layer panel was created, with dimensions of 3 m in width, 2 m in height, and a thickness of 0.12 m, as shown in Fig. 4. The maximum mass per unit area for the fabricated panels was

approximately 165 kg/m². The ballistic protection panel as it is described in the Moldovan et al. [15] and depicted in Fig. 4 has its supporting structure composed of a metal frame (1) on which the protective layers (2) are arranged, the entire assembly being supported by a transport and fixation system (3). The protective layers (2) consist of a blast steel slag layer (5) with a thickness of 10 cm, and each assembly contains 10 layers of Dyneema (4) and a Tego plate (6) on each side of the slag layer (2).

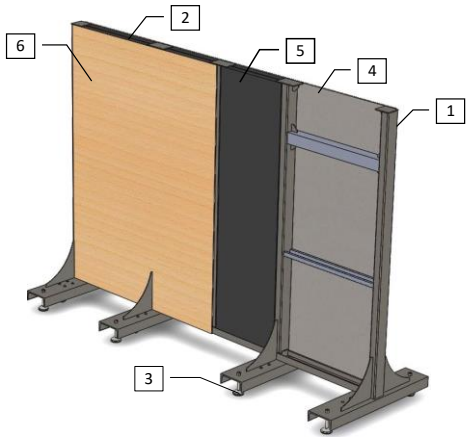

Fig. 4. Structure and configuration of the multi-layer ballistic protection panel testing setup: 1 - metal frame; 2 – layers of various materials; 3 - transport and fixation system; 4 – two assemblies consisting of ten layers of Dyneema fabric symmetrically arranged on the exterior relative to the median plane of the ballistic panel; 5 – blast steel slag layer; and 6 – Tego plates [15]

To test the behaviour of the multi-layer ballistic panel under the effects of the explosion of an IED, an explosive device consisting of a 5 kg equivalent TNT plastic explosive charge was used, positioned 1 m away from the panel and at a height of 0.6 m above the ground. On one face of the parallelepiped-shaped explosive charge, steel balls with a diameter of 10 mm were arranged, as shown in Fig. 2b.

2.5 Test setup for fragments and bullets velocity mitigation

To determine the mitigation capacity of the velocity of metal balls and projectiles, the impact velocity and the velocity remaining after penetration of the multi-layer panels, Dyneema layers, or granular material layers were measured. The measurement of impact velocity and residual velocity after penetration was carried out using a ballistic radar, following NIJ 0101.06 standard recommendations, and an ultra-high-speed FASTCAM SA-X2 type 1080-C3 camera, as shown in Fig. 2a.

For the tests, two types of fragments and projectiles were selected: a) deformable (HPBT bullets) and b) non-deformable (ball bearings and FMJ bullets). Among the potential fragments, steel balls were preferred due to their spherical shape and homogeneity compared to other fragment types. The diameter of the steel

balls used for the tests was 8 mm and 10 mm. However, the use of metal balls for testing the panels' mitigation capacity did not ensure test repeatability, and therefore, 7.62 mm bullets were also used. The initial velocities of the bullets were 785 m/s for HPBT ammunition and 860 m/s for FMJ ammunition, while the impact velocity of the balls was 726 m/s for 8 mm balls and 526 m/s for 10 mm balls. Additional information regarding the characteristics of the ammunition used and the configuration of the explosive devices used for propelling the balls can be found in the paper Iftimie et al. [9].

To measure the pressure in the shock wave front, three pressure sensors were used, as shown in Fig. 2b: S1 - PCB 102B15 (measuring range (MS): 1.379 kPa, sensitivity (Sen.): 3.6 mV / kPa) to measure the side-on pressure, and S2 - PCB PCB 113B24 (MS: 6895 kPa, Sen.: 0.725 mV/kPa), and S3 - PCB 113B26 (MS: 3450 kPa, Sen.: 1.45 mV/kPa) to measure reflected pressure. Sensor S1 was placed on the side of the multi-layer ballistic panel at a distance of 5 m, and sensors S2 and S3 behind the panel at distances of 1.5 m and 4 m, respectively. The sensors were connected to a Genesis type GEN7I-2 high-speed data acquisition system with a sampling rate of 2 MS/s.

3. Results and Discussions

3.1 Impact velocity determination for FMJ and HPBT ammunition

For conducting tests regarding the attenuation capacity of various materials, FMJ and HPBT ammunition types were used. These were fired remotely, and the velocity before impact was measured using ballistic radar. The results are presented in Fig. 5.

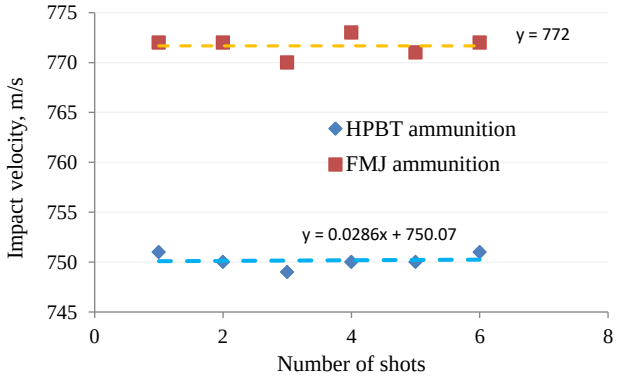

Fig. 5. Impact velocity of the projectiles used for testing

The variation in impact velocities of the projectiles is attributed to the conditions on the day of the tests. In calculating the attenuation produced by different materials, the average values of projectile velocities at impact with the

panels will be considered for the two ammunition types, namely 750 m/s for HPBT ammunition and 772 m/s for FMJ ammunition.

3.2 The influence of the type and granulation of the granular material

The influence of the type of granular material on its capacity to attenuate 7.62 mm calibre ammunition, HPBT (deformable), and FMJ (non-deformable) types is depicted in Fig. 6. For HPBT ammunition, two sand and three slag sorts were used for tests, while for FMJ ammunition tests the same sand sorts were used, but for the slag only the best two sorts in terms of attenuation in tests with HPBT ammunition. In the case of HPBT ammunition, it was observed that steel slag is a better attenuator than sand, regardless of the particle size of the granular material.

Additionally, it can be observed that the projectile attenuation improves as the particle size decreases for the same type of granular material, whether it is sand or slag. However, it has been noted that bulk granular materials have a better attenuation capacity than those with finer granulation. Thus, attenuation for the sand fraction with particle sizes between 0.4 mm and 0.8 mm is lower by percentages ranging between 13% and 15% compared to the sand fraction with particle sizes smaller than 1 mm. Moreover, it is found that the slag fraction with particles smaller than 2 mm does not provide as effective attenuation as bulk slag or that with particle sizes between 2 mm and 4 mm. The explanation may be that finer particles have a more regular shape, and the relative displacement of granular material particles and the resulting friction between particles are reduced compared to cases where particles have larger and irregular shapes. For bulk materials, smaller particles contribute to filling the gaps between larger particles, thereby increasing friction between particles. Thus, it is observed from Fig. 6a that only the slag fraction with particle sizes between 2 mm and 4 mm exhibits better attenuation than bulk slag.

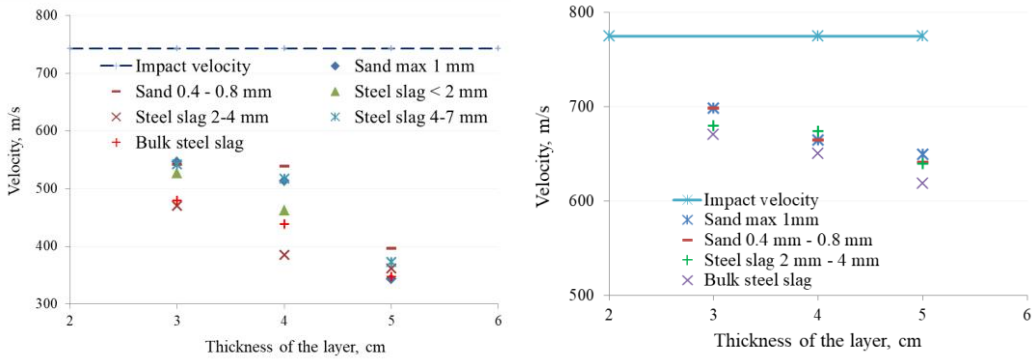

a) HPBT 7.62 mm bullets b) FMJ 7.62 mm bullets

Fig. 6. The influence of the type and thickness of the granular material layer on the attenuation of the velocity of 7.62 mm calibre ammunition

Increasing the thickness of the granular material layer leads to an increase in projectile velocity attenuation, regardless of the granular material or granulation, as it can be seen in the Fig. 6. In the case of FMJ ammunition, as shown in Fig. 6b, it is observed that regarding sand, the particle size does not have a significant impact on projectile velocity attenuation, with values ranging between 10% and 17% relative to the impact velocity, depending on the thickness of the material layer.

On the other hand, fine-grained slag, with particle sizes between 2 mm and 4 mm, exhibits a behaviour similar to sand. In contrast, bulk slag provides the best projectile velocity attenuation for the tested granular material layer sizes, with the maximum value of projectile velocity attenuation reaching 20% for a granular material thickness of 5 cm.

The firings conducted on thicknesses of granular material, namely sand with particle sizes ranging from 0.4 mm to 0.8 mm and bulk slag from 5 cm to 20 cm, allowed to determinate the thickness value of the granular material layer at which the residual velocity is zero, as shown in Fig. 7. It is observed that for thicknesses up to 10 cm of the granular material layer, the difference in attenuation produced by bulk slag and sand with particle sizes between 4 mm and 8 mm is at a maximum of 10%. Beyond this thickness of the granular material, the difference increases to 36% at a thickness of 15 cm and reaches approximately 80% at an 18 cm thickness of the granular material.

The data presented in Fig. 7a for sand corresponds to those presented by Børvik et al. in [13]. Hence, for dry sand, Børvik et al. determined that the thickness of the layer required for the residual velocity of a 7.62 mm FMJ bullet to reach zero is approximately 200 mm. For a ballistic panel designed to attenuate the effects resulting from the explosion of an IED, it is of interest to determine the attenuation capacity for fragments and splinters of various shapes and sizes.

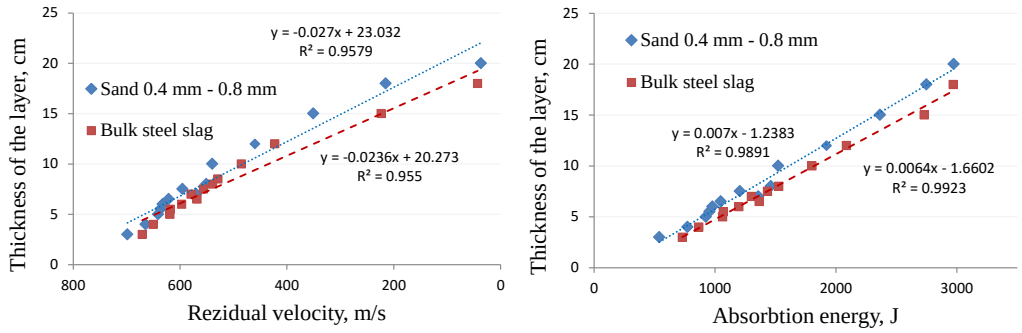

a) b)

Fig. 7. The variation of residual velocity (a) and absorbed energy (b) of the 7.62 mm FMJ bullet as a function of the thickness of the sand and slag layer

As stated in paragraph 2, metallic balls with diameters of 8 mm and 10 mm were used for tests to simulate fragments and splinters propelled by an IED explosion. Literature data indicate that for metallic balls, the ballistic limit is 258 m/s compared to 181 m/s for conical nose shape projectiles, similar to FMJ ammunition as is described by Chian et al. in [14]. The ballistic limit represents the impact velocity on a target of a certain material at which the residual velocity of the projectile is zero. In the case of a ballistic protection panel, the main concern is to determine which granular materials are used so that, together with Dyneema layers, they provide the maximum attenuation of projectile velocities. For a ballistic protection panel, the primary consideration is identifying the granular materials that, when combined with Dyneema layers, offer the most effective reduction in projectile velocities.

If the absorbed energy is defined as the difference between the kinetic energy of the projectile before and after passing through the granular material layer, comparisons can be made with data available in the literature regarding the influence of the shape and velocity of the projectile. The graphical representation of the variation in energy absorbed by layers of sand and slag as a function of their thickness is presented in Fig. 7b. It is observed that at the same thickness of the granular material layer, slag has a higher capacity for projectile energy attenuation (absorption) than sand (reduces the residual velocity of the projectile).

According to Chain et al. [14], the variation of energy absorbed by sand for projectiles with conical, hemispherical, or flat nose shapes, as a function of impact velocity, is described by the relationships:

$$E_a = \left(v_{impact} - 196.14\right)/0.196 \text{ [J], for a projectile mass of 15 g,} \quad (1)$$

$$E_a = \left(v_{impact} - 163.06\right)/0.1623 \text{ [J], for a projectile mass of 20 g,} \quad (2)$$

while for spherical–nosed projectiles, with a mass of 7 g, the relation is as follows:

$$E_a = \left(v_{impact} - 138.78\right)/0.4097 \text{ [J]} \quad (3)$$

where v_{impact} is the impact velocity of the projectile.

The graphical representation of these equations is presented in Fig. 8 and indicates that at the same value of projectile impact velocity, the absorbed energy is higher for projectiles with greater mass, being almost double for the 15 g mass projectile compared to the 7 g one.

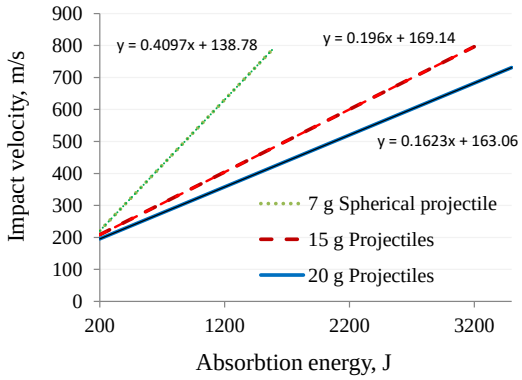

Fig. 8. The variation of impact velocity as a function of absorbed energy for projectiles of different shapes and masses as depicted in [14]

The analysis of the graph in Fig. 7b indicates that for a blast steel slag layer with a thickness of 18 cm, almost complete attenuation of a FMJ 7.62 mm projectile with an impact velocity of 772 m/s and a mass of 10.7 g is achieved. The absorbed energy for attenuating this velocity is approximately 3000 J.

From Fig. 8, it is observed that for this impact velocity and a mass of a spherical projectile of 15 g, an absorbed energy of about 3000 J corresponds to approximately half the absorbed energy for a spherical projectile with a mass of 7 g. This comparison demonstrates that a layer of approximately 10 cm of loose blast steel slag can attenuate the velocity of a 10 cm diameter metal ball with a mass of approximately 4 g.

3.3 The influence of Dyneema layers

Tests were conducted to determine the mitigation capacity of an assembly consisting of 6 or 12 layers of Dyneema fabric arranged on wooden panels, as shown in Fig. 3d, against 10 mm diameter metal balls. The explosive device was placed at a distance of 50 cm from the panel. The 50 cm distance was chosen to minimize the dispersion of metal balls before the panel and ensure a maximum number of balls impacting the panel. The disadvantage of placing the explosive device at such a distance from the panel is that high-speed camera filming to determine the residual velocity of the balls after perforating the Dyneema layers is not possible. The results of the tests show that in both cases, the 10 mm diameter metal balls penetrated the assembly of Dyneema layers, with no significant differences observed in the behaviour between the two assemblies of 6 and 12 Dyneema layers, as depicted in Fig. 9. The only notable differences between the two cases relate to the level of delamination on the back surface of the 12-layer Dyneema assembly, which is lower than that for the case with 6 layers.

a) b) c) d)

i) Effects on the front (a) and back (b) sides of the assembly consisting of 6 layers of Dyneema fabric

ii) effects on the front (c) and back (d) sides of the assembly consisting of 12 layers of Dyneema fabric

Fig. 9. The effects of 10 mm diameter metal balls on 6 layers (i) and 12 layers (ii) of Dyneema fabric

The tests conducted with 7.62 FMJ ammunition on 6 or 12 layers of Dyneema showed insignificant attenuation. However, the introduction of two assemblies consisting of 12 layers of Dyneema fabric on either side of a layer of bulk slag with varying thicknesses results in a reduction of residual velocity between 3% and 7%, as shown in Fig. 10.

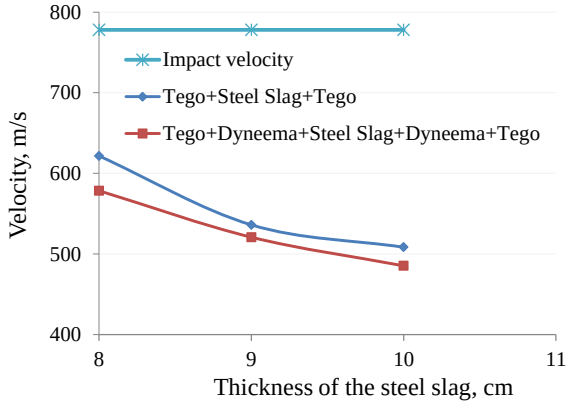

Fig. 10. The influence of Dyneema layers on the attenuation of 7.62 mm FMJ bullets

3.4 Results from experiments conducted on actual multi-layered ballistic panels

Tests were conducted on two multi-layered ballistic panels, the shape and composition of which are presented in Fig. 4. The results obtained from the tests are depicted in Fig. 11.

a) The front face of the panel before and after removing the Tego plate

b) The back face of the panel before and after removing the Tego plates

Fig. 11. The effects of the metal balls on the multi-layered ballistic panel

On the front face, traces of penetration by the metal spheres can be observed through the Tego plate and then through the first assembly consisting of layers of Dyneema fabric. This assembly, in turn, was completely perforated by the metal spheres, as shown in Fig. 11a. However, on the rear face, no perforations were recorded either at the level of the Dyneema layers or at the level of the Tego plate, as illustrated in Fig. 11b. These results demonstrate that the configuration with a 10 cm thick layer of loose slag and two assemblies of 12 layers of Dyneema fabric arranged on either side of the granular material layer ensures the attenuation of 10 cm diameter metal spheres propelled by an explosive charge of approximately 5 kg TNT equivalent.

To verify the shock wave propagation and overpressure values, the configuration presented in Fig. 2b was used. The recorded overpressure values are presented in Table 2.

To compare the maximum values of shock wave overpressure resulting from the experimental tests (Fig. 12) with theoretical values, the calculation relationships of both Kinney [16] and Kingery-Bulmash [17] were employed.

$$\Delta p_f = P_0 \frac{808 \cdot \left[1+\left(\frac{Z}{4.5}\right)^2\right]}{\sqrt{1+\left(\frac{Z}{0.048}\right)^2}\cdot\sqrt{1+\left(\frac{Z}{0.32}\right)^2}\cdot\sqrt{1+\left(\frac{Z}{1.35}\right)^2}}, \text{ [bar]} \tag{4}$$

$$\Delta p_f = Exp(A + B\cdot\ln Z + C\cdot(\ln Z)^2 + D\cdot(\ln Z)^3 + E\cdot(\ln Z)^4), \text{ [kPa]}. \tag{5}$$

In the above equations, P_0 represents atmospheric pressure (bars), and Z represents the scaled distance.

$$Z = \frac{R}{W^{1/3}}, \text{ [m/kg}^{1/3}\text{]}, \tag{6}$$

where *R* is the distance from the explosive charge to the target, *W* is the quantity of TNT equivalent explosive, and A, B, C, D, and E are constants whose values are specified by Kingery and Bulmash in the paper [17].

Table 2

Values of the side-on and reflected pressure calculated using Kinney and Kingery-Bulmash equations and the experimentally determined values

Method	Standoff distance (m)			
	2.5		5	
	Pressure, (MPa)			
	Side-on	Reflected	Side-on	Reflected
Experimental	-	2.770	0.158	0.332
Kinney	0.431	1.939	0.087	0.333
Kingery-Bulmash	0.585	2.715	0.122	0.354

The variation of pressure over time presented in Fig. 12 for the three sensors in Fig. 2b can be explained using the high-speed camera recordings.
It should be noted that the calculated incident pressure value using the Kinney relationship corresponds to the case where the shock wave has not encountered any obstacle, and the reflected pressure value was calculated using the Rankine-Hugoniot equations. The incident and reflected pressure values according to Kingery-Bulmash correspond to the case of a hemispherical explosion, where a Mach stem is formed.

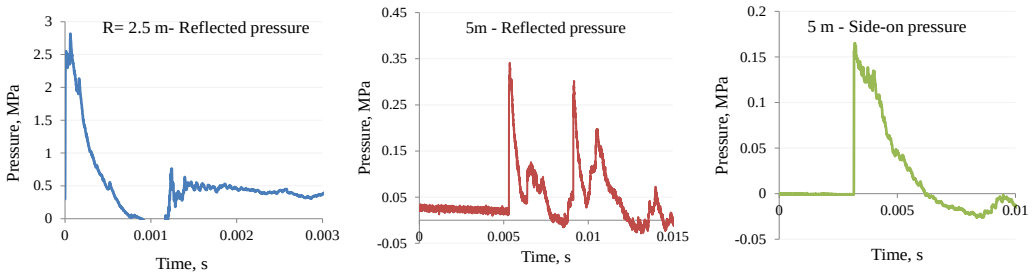

a) b) c)

Fig. 12. The variation of pressure over time for the sensors presented in Fig. 2b

Thus, the orientation of sensor S1 was set to record the incident pressure. However, due to the large distance between the explosive charge and this sensor, the recorded value corresponds to the pressure in the front of a Mach stem, as observed from the values presented in Table 2 and Fig. 12c. The shock wave generated by the explosive charge reflects off the panel and ground, passes under the panel, and heads towards sensor S2, as shown in Fig. 13b, with the recorded pressure presented in Fig. 12a. This front will propagate further, causing the first peak in the pressure curve in Fig. 12b, with subsequent peaks resulting from shock waves passing over and around the panel.

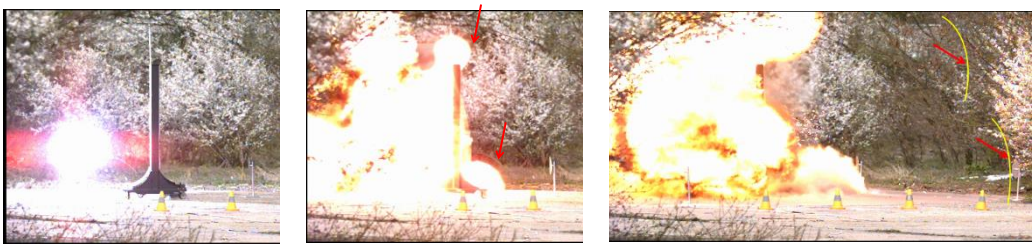

a) detonation of the explosive charge

b) Mach stem (bottom) and shock wave passing over the panel (top)

c) evolution of shockwave fronts when Mach stem reached sensor S3

Fig. 13. Propagation of shock waves resulting from the explosion of the explosive charge (red arrows indicate the position of the shock waves)

The graphs in Fig. 12 and the images presented in Fig.13 indicate that although the panel does not allow the initial shock wave from the explosive charge to pass through, shock waves circumventing the panel at the bottom, top, and sides will reach behind it, and their effects can be significant.

4. Conclusions

To determine the attenuation capacity of the shock wave effects and the propulsion of fragments and srapnels resulting from the explosion of an IED, a multi-layer ballistic panel was developed. The panel configuration consists of a central layer of granular material and two assemblies formed by layers of Dyneema fabric arranged on either side of the central layer. For the granular material, the choice was made between two sorts of sand (with particle sizes ranging from 0.4 to 0.8 mm and particles with sizes up to 1 mm) and four sorts of blast steel slag (bulk slag, slag with particle sizes smaller than 2 mm, with particle sizes ranging from 2 to 4 mm, and particle sizes ranging from 4 to 7 mm).

The results of tests conducted on these sorts and types of granular materials have shown that the best attenuation capacities for FMJ and HPBT 7.62 mm bullets are achieved with sand having particle sizes between 0.4 and 0.8 mm and bulk slag.

Subsequent experimental research conducted on panels made of these granular materials allowed the determination of the residual velocity and absorbed energy in relation to the thickness of the granular material layer. It was observed that bulk slag exhibits a better attenuation capacity up to 8%.

Using data from the specialized literature regarding the dependence of absorbed energy on the projectile nose shape and impact velocity, it was determined that a thickness of approximately 10 cm of bulk slag would be suitable for attenuating metal balls up to 10 cm in diameter. The use of two assemblies consisting of 10 layers of Dyneema fabric resulted in a reduction of residual projectile velocities ranging from 3 to 7%.

The experimental tests conducted on real-sized multi-layered ballistic panels have confirmed its ability to successfully attenuate fragments that may be generated from the explosion of an IED. The experimental tests have shown that, although the panel does not allow the initial shock wave from the explosive charge to pass through, shock waves that bypass the panel from the bottom, top, and sides will reach behind it, and their effects can be significant depending on the amount of explosive material in the IED.

Acknowledgments

The work was partially supported by the FSI - EU grant RO FSIP2016 OS6A12P01.

R E F E R E N C E S

[1]. *A. Ramasamy, A.M. Hill, J.C. Clasper*, Improvised explosive devices: pathophysiology, injury profiles and current medical management, Journal of Army Medical Corps, **vol. 155**, no. 4, 2009, pp. 65-272.
[2]. *J.L. Arnold, P. Halpern, M.C. Tsai, H. Smithline*, Mass casualty terrorist bombings: a comparison of outcomes by bombing type, Ann. Emerg. Med., **vol. 43**, no. 2, 2004, pp. 263-273.
[3]. *R. Golan, D. Soffer, A. Givon, K. Peleg*, The ins and outs of terrorist bus explosions: Injury profiles of on-board explosions versus explosions occurring adjacent to a bus, Injury, **vol. 45**, no. 1, 2014, pp. 39-43.
[4]. *A.C. Doctor, S. Hunter*, The Future of Terrorist Use of Improvised Explosive Devices: Getting in Front of an Evolving Threat, CTCSentinel, **vol. 16**, no 11, 2023, pp. 41-51
[5]. *V. Karlos, M. Larcher, G. Solomos*, Review on soft target/public space protection guidance, EUR, ISBN 978-92-79-79907-5, 2018, doi: 10.2760/553545.
[6]. *D. Bianchini*, Person-Borne Improvised Explosive Devices, Symposium on Innovation in Aviation Security, Montréal, Canada, 21-23 October 2014.
[7]. *S. S. Ateş, M. Uzulmez*, Terrorist attacks in aviation: an analysis of Ataturk airport attack on, Pressacademia, **vol. 3**, no 1, 2017, pp. 1012-1018.
[8]. *A. Cuesta, O. Abreu, A. Balboa, D. Alvear*, A new approach to protect soft-targets from terrorist attack, Safety Science, **vol. 120**, 2019, pp. 877-885.
[9]. *B. Iftimie, M. Lupoae, O. Orban*, Experimental Investigations Regarding the Behaviour of Composite Panels Based on Polyurea and Kevlar or Dyneema Layers Under Blast and Fragments, Revista de Materiale Plastice, **vol. 56**, no. 3, 2019, pp. 538-542.
[10]. *B. Iftimie, M. Lupoae, E. Trană*, Aspects of determining impact induced shock characteristics in multilayered ballistic panel materials, U.P.B. Sci. Bull., Series B, **vol. 85**, no. 3, 2023, pp. 155-166.
[11]. *M. Omidvar, M. Iskander, S. Bless*, Response of granular media to rapid penetration, Int. J. of Impact Engineering, **vol. 66**, 2014, pp. 60-82.
[12]. *M.E. Backman, W. Goldsmith*, The mechanics of penetration of projectiles into targets, Int. J. of Engineering Sci, **vol. 16**, 1978, pp. 1-99.
[13]. *T. Børvik, S. Dey, L. Olovsson*, Penetration of granular materials by small-arms bullets, Int. J. of Impact Engineering, **vol. 75**, 2015, pp. 123-139.
[14]. *S.C. Chian, V.B.C. Tan, A. Sarma*, Projectile penetration into sand: Relative density of sand and projectile nose shape and mass, Int. J. Impact Engineering, **vol. 103**, 2017, pp. 29-37.

[15]. *M. Moldovan, B. Iftimie, C. Bogorin, M. Lupoae, O. Orban*, Ballistic protection pannel, OSIM Patent no 133792, 2021.
[16]. *G.F. Kinney, K.J. Grahm*, Explosive shocks in air, Springer, Berlin, 1985.
[17]. *C.N. Kingery, G. Bulmash*, Airblast parameters from TNT spherical air burst and hemispherical surface burst. US Army Armament Research and Development Center, Ballistics Research Laboratory, Aberdeen Proving Ground, Maryland, USA, Technical Report ARBRLTR-02555, 1984.